Geol. Mag. **139** (*4*), *2002, pp. 437–452.* © *2002 Cambridge University Press*
DOI: 10.1017/S0016756802006684 *Printed in the United Kingdom*

Picritic magmas and the Rum ultramafic complex, Scotland

B. G. J. UPTON*†, A. C. SKOVGAARD‡, J. McCLURG*, L. KIRSTEIN*, M. CHEADLE§, C. H. EMELEUS¶, W. J. WADSWORTH|| & A. E. FALLICK#

*Department of Geology and Geophysics, Edinburgh University, EH9 3JW, UK
‡Danish Lithosphere Centre, Copenhagen, DK-1350, Denmark
§Department of Geology and Geophysics, University of Wyoming, Laramie, Wyoming, 82071, USA
¶Department of Geological Sciences, Durham University, Durham, DH1 3LE, UK
||Department of Geology, Manchester University, Manchester, M13 9PL, UK
#Scottish Universities Environmental Research Centre, East Kilbride, G75 0QF, UK

(*Received* 7 August 2001; *accepted* 17 April 2002)

Abstract – Three small picritic dykes, intruded at a late stage in the evolution of the Rum basic–ultrabasic complex, Inner Hebrides, shed new light on the nature of the magmas responsible for the main complex. The magmas are of transitional (mildly alkalic) type, generated by relatively small-fraction (6–7%) melting of a depleted mantle source. Melting is tentatively deduced to have commenced at ± 100 km, straddling the garnet–spinel transition. Of the three samples, one (M9) is remarkable for the preservation of very primitive characteristics, with olivines of Fo_{93} containing highly aluminous spinels; these appear unique within the British Tertiary Volcanic Province. Sr, Nd and Pb isotopes indicate only minor (≤4%) contamination with Precambrian crustal lithologies, reflecting the rapidity of ascent of the magma batches. The Rum picrites have $^{187}Os/^{188}Os$ ratios and trace element characteristics comparable to those of recent picrites from Iceland, suggesting minimal temporal change of the depleted parts of the Iceland plume over 60 Ma. Movements of the Long Loch Fault may have been instrumental in causing decompression melting of the spreading Iceland plume-head and facilitating ascent of the melts to near-surface levels.

Keywords: picrite, magmas, Iceland, mantle, plumes.

1. Introduction

The early Tertiary igneous complex on the island of Rum in the Inner Hebrides of Scotland has been the subject of a large number of studies during the past forty years (see Emeleus *et al.* 1996; Emeleus, 1997, and references therein). The complex was emplaced over a period of *c*. 1 m.y. at 60.5 Ma (Hamilton *et al.* 1998) and involved dacitic and microgranitic rocks ('felsites and granophyres') in its early stages (Troll, Emeleus & Donalson, 2000) and gabbroic and peridotitic rocks in its later stages. The latter rocks compose the shallow-crustal, layered cumulate successions for which the island is celebrated. These successions have been subdivided into: (1) the Eastern Layered Series, (2) the Western Layered Series and (3) the Central Series. The Eastern and Western Layered Series were probably originally contiguous but are separated by the Central Series within which some stratigraphically higher and younger cumulates may be represented. Additionally, gabbroic and peridotitic rocks occur as apophyses extending to the north of the main complex as well as in numerous plugs (J. McClurg, unpub. Ph.D. thesis, Univ. Edinburgh, 1982; J. A. Volker, unpub. Ph.D. thesis, Univ. Edinburgh, 1983; Wadsworth, 1994). Some of the apophyses and plugs cross-cut the main gabbro–peridotite massif whilst others intrude the Precambrian country rocks away from the central complex (Fig. 1).

Numerous authors have debated the composition of the magmas from which the Rum layered complex crystallized. Because of extensive contact hybridization with silicic wall-rocks, analyses of uncontaminated chilled facies do not provide a satisfactory answer to this vexed question, although Greenwood, Donaldson & Emeleus (1990) described what might approximate to a chilled facies of the Eastern Layered Series. Brown (1956) considered the Eastern Layered Series to have been produced from repetitive influxes of an aluminous tholeiitic basalt magma. Donaldson (1975) and Gibb (1976) were more precise in suggesting that olivine 'eucrite' magmas were responsible. McClurg (J. McClurg, unpub. Ph.D. thesis, Univ. Edinburgh, 1982) and Kent (1995), recognizing that highly magnesian magmas must have been involved in the crystallization of so large a volume of cumulates dominated by forsteritic olivine, used the terms 'picrite' and 'magnesian basalt' respectively for the parental magmas. A parental magma consisting of an olivine tholeiitic liquid carrying olivine crystals (*c.* 19% modal) in suspension was deduced by Greenwood, Donaldson & Emeleus (1990) from their investigation of the chilled margin of the Eastern

† Author for correspondence: bupton@glg.ed.ac.uk

Layered Series. However, the problem of likely wall-rock contamination of this marginal sample remains unclear as it indicates a tholeiitic picrite rather than a transitional or mildly alkaline one as has been argued by McClurg (J. McClurg, unpub. Ph.D. thesis, Univ. Edinburgh, 1982) and Kitchen (1985).

The present paper concerns three small picritic dykes, intruded within the ultrabasic complex late in its history, well-removed from the contacts of the complex and relatively close (0.9–1.6 km) to the Long Loch Fault zone which is suspected to overlie the principal conduit through which magma was supplied to the developing complex (J. McClurg, unpub. Ph.D. thesis, Univ. Edinburgh, 1982; Emeleus *et al.* 1996). It is suggested that these dykes represent rapidly cooled products of late-stage, small-volume magma batches compositionally similar to the preceding, much larger, batches from which the layered cumulates crystallized.

The petrology of the cumulates and the compositions of the chilled margin and small dykes indicate that highly magnesian melts, which ascended to within one or two kilometres of the surface before either freezing or fractionating to more evolved compositions, produced the layered complex (Emeleus *et al.* 1996). Contact metamorphism and partial melting of country rocks, the evidence for a prolonged cooling history and the fact that the complex is dominantly composed of peridotitic rocks, imply that the parental magmas were (a) high temperature and (b) highly magnesian. According to Emeleus *et al.* (1996) the mean parental magma must have contained approximately 18 ± 2 wt% MgO. The magmas are likely to have been variably fractionated with respect to olivine depending on their ascent and cooling rates. Olivine compositions within the coarse plutonic rocks are rarely more magnesian than Fo_{90} (J. A. Volker, unpub. Ph.D. thesis, Univ. Edinburgh, 1983), although olivine-rich sands eroded from the complex and dredged off the southern coast have a range of $Fo_{92–80}$ (Gallagher *et al.* 1989). The 'plutonic' olivines are unzoned and have probably undergone sub-solidus re-equilibration. Consequently it is unlikely that original 'magmatic' compositions are retained.

Whereas the sequence of crystallization seen in the layered complex was (1) olivine, (2) plagioclase and (3) clinopyroxene, the silica activity of the magmas was insufficient for crystallization of low-Ca pyroxenes. The pyroxenes of the layered cumulates have high Ca, Ti, Al and limited Fe enrichment pointing to an alkali affinity and plots of Si vs. Al^{IV} and TiO_2 vs. Al^{IV} show that the majority of data points fall in the transitional alkaline fields (J. McClurg, unpub. Ph.D. thesis, Univ. Edinburgh, 1982). Furthermore, vein segregations within the Rum peridotites have distinctly alkaline characteristics (Kitchen, 1985; Faithfull, 1985) consistent with the thesis that the parental magmas were transitionally alkalic rather than tholeiitic.

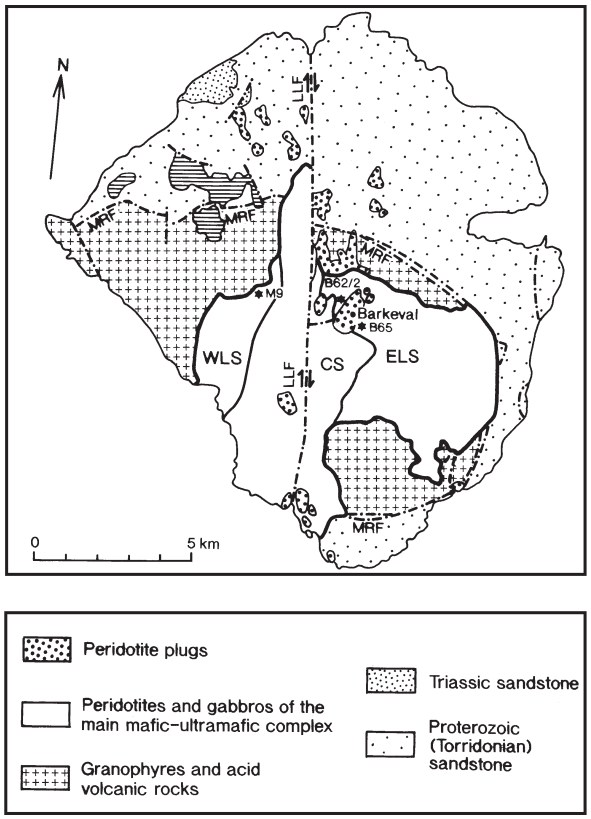

Figure 1. Sketch map of the geology of Rum showing locations of the three picritic samples. MRF, Main Ring Fault. WLS, Western Layered Series. CS, Central Series. ELS Eastern Layered Series. LLF, Long Loch Fault. Sample collection sites indicated by stars.

2. Picritic dykes

Large numbers of minor intrusions occur on Rum (Emeleus, 1997) among which mafic dykes are abundant (R. M. Forster, unpub. Ph.D. thesis, Univ. Durham, 1980; Speight *et al.* 1982). The least evolved of these (namely the picrites and some of the olivine dolerites) cut the central complex and form part of a radial dyke swarm. Forster subdivided the minor intrusions into twelve groups of which his Group 1 comprises picritic dykes which, relative to the great majority of the hypabyssal intrusions, were intruded late. Forster's Group 1 dykes are olivine-phyric with bulk MgO up to 31 wt%. Most of the dykes, however, are of transitional basalt compositions; these cut the early felsic units of the central complex, but few post-date the gabbro–peridotite complex. Forster's Group 2 dykes, which are either aphyric or sparsely porphyritic with olivine and/or plagioclase phenocrysts, are themselves relatively magnesian with 11–14 wt% MgO. The picritic dykes tend to be small (< 1 m width) and olivine-phyric but with highly variable phenocryst contents. McClurg (J. McClurg, unpub. Ph.D. thesis, Univ. Edinburgh, 1982) described in detail some small picritic dykes occurring mainly on the south and west flanks of Barkeval (Fig. 1) which post-date the hetero-

https://doi.org/10.1017/S0016756802006684 Published online by Cambridge University Press

geneous gabbro plugs which, in turn, intrude the layered suite. She noted that there may be up to four generations of such dykes, the youngest of which are truncated, and thermally metamorphosed by the large, late-stage peridotite plug on Barkeval. Whilst the olivines are 'fresh', they contain a dusting of iron-oxide particles. The matrices of the dykes consist of olivines and zoned plagioclases enclosed by brown clinopyroxene and variable amounts of strongly pleochroic red brown/honey-coloured pargasitic amphibole. There are also abundant blebs of sulphides (chalcopyrite, pyrrhotite and pentlandite, inferred to have crystallized from homogeneous monosulphide globules), often enclosed by ilmenite and magnetite.

The occurrence of primary pargasite and, more rarely, phlogopite, characterizes some of the picrites and indicates that the melts evolved towards Ti-rich undersaturated residues. The presence of groundmass olivine and brown (titaniferous) pyroxene further confirms the alkalic affinities. The relative abundance of sulphide droplets suggests that the melts were sulphur-saturated just before and immediately after emplacement.

McClurg (J. McClurg, unpub. Ph.D. thesis, Univ. Edinburgh, 1982) subdivided the picritic dykes into three groups:

Group 1: Dykes containing 10–40% olivine phenocrysts which are generally equant and between 0.5 and 5 mm diameter. The compositional range of the olivines is $Fo_{83.8–79.9}$. They are accompanied by spinel microphenocrysts up to 0.6 mm across. The dyke matrices contain small quantities of amphibole and/or phlogopite.

Group 2: Picritic dykes which cut, and are occasionally cut by, Group 1 dykes. They lack primary amphibole (and mica) but are otherwise petrographically similar to the Group 1 picrites. The compositional range for the olivines is $Fo_{77.0–72.5}$. The matrices contain zoned plagioclase, sub-ophitic brown clinopyroxene, primary ilmenite and magnetite (in an approximately 1 : 1 ratio) and composite sulphide globules.

Group 3: This group comprises a few, small (10–20 cm wide) sinuous and black-weathering dykes. They lack chilled margins and indications of flow-differentiation. They are very olivine-rich and contain appreciable contents of modal spinel.

3. Analytical methods

Mineral and whole-rock analyses were made at the Department of Geology and Geophysics, University of Edinburgh. Olivines and oxides were analysed on a Cambridge Scientific Instruments Microscan 5 microanalyser, using the wavelength dispersive method. Pure elements, oxides and simple silicate compositions were used as standards. Corrections were made for dead-time, atomic number, absorption and fluorescence using computer programs based on methods by Sweatman & Long (1969). The operating conditions were 20 kV and a sample current of 30 nA.

Whole-rock XRF analyses were made using a Philips PW 1480 spectrometer equipped with a Rh-anode X-ray tube. The instrument was calibrated using CRPG and USGS reference standards (Govindaraju, 1994). Major elements were determined on fused glass discs (Norrish & Hutton, 1969) with corrections applied for inter-element mass absorption effects. A full description of the techniques used is given in Fitton *et al.* (1998). Rare-earth elements (REE) were analysed by ICP-AES at the Department of Geology, Royal Holloway, University of London, following the method of Walsh, Buckley & Barker (1981).

4. Petrography and mineralogy of the three dykes

This paper presents data from three of the small picritic dykes, with strongly contrasting textures, described by McClurg (J. McClurg, unpub. Ph.D. thesis, Univ. Edinburgh, 1982) and represent each of her three groups. Two of the dykes (samples B62/2 and B65) are from the Atlantic Corrie Wall of Barkeval, near Bealach Bairc-Meall (Fig. 1) in the Eastern Layered Series whereas M9 is from a dyke that cuts the Western Layered Series close to its western margin. Representative analyses of olivines and oxides from the samples are presented in Table 1.

4.a. Sample B62/2

B62/2 comes from a Group 1 dyke containing approximately 10% modal olivine phenocrysts in a fine-grained granular matrix (Fig. 2a). The olivines are euhedral to subhedral, up to 8 mm in diameter with some normal zoning ($Fo_{85.9–80.5}$), typically cloudy with fine, hair-like or comb-like opaque inclusions. The matrix comprises plagioclase, augite, olivine, opaque spinel with minor amounts of amphibole and/or mica.

4.b. Sample B65

Sample B65 is a textural variant within Group 2. It lacks olivine phenocrysts and was regarded by McClurg as an 'all-liquid quench' product. B65 has a coarse spinifex-type quench texture involving skeletal olivines up to 12 mm long, with subhedral plagioclase crystals (up to 5 mm), interstitial pale brown augite containing finely exsolved needles of rutile and small subhedra of opaque spinel (Fig. 2b). The approximate mode is 35% ol, 35% plag, 25% cpx and 5% opaque minerals. The olivines in B65 comprise delicate hopper and crystallographic branching morphologies (Donaldson, 1976). The crystals have random orientation and the majority are unbroken. It should be emphasized that the olivines ($Fo_{77–74.5}$), do not repre-

https://doi.org/10.1017/S0016756802006684 Published online by Cambridge University Press

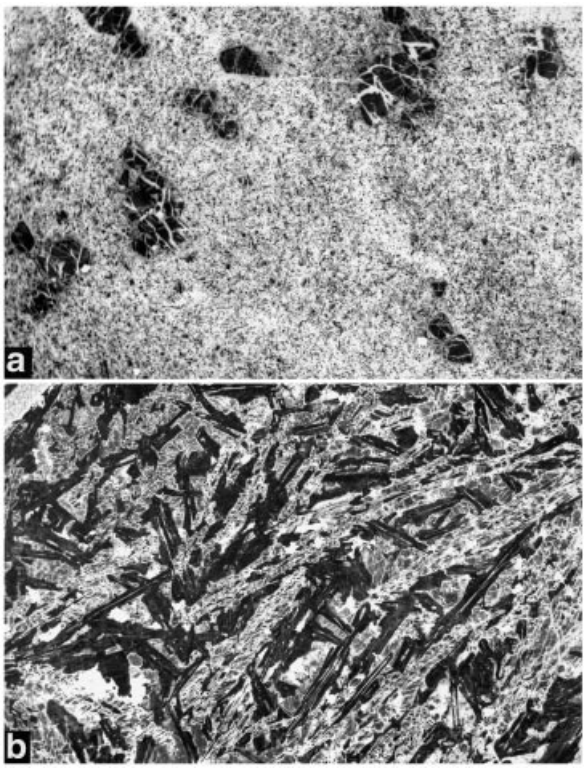

Figure 2. (a) Photomicrograph of B62/2 showing olivine phenocrysts in a fine-grained matrix. Field-width ~15 mm. (b) Photomicrograph of B65 showing 'spinifex-type' quench texture. Field-width ~8 mm.

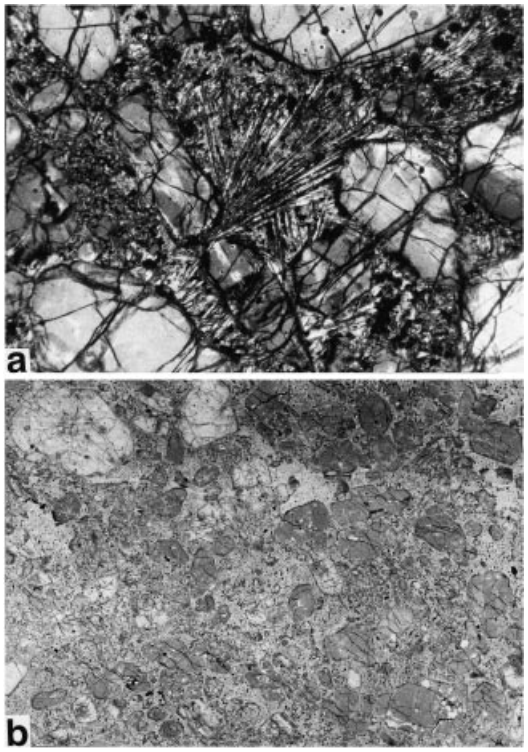

Figure 3. (a) Photomicrograph of M9 showing quench sprays of olivine and pyroxene in the matrix. Field-width ~4 mm. (b) Photomicrograph of M9 showing Type A (cloudy brown) and Type B (colourless) olivine crystals in a fine-grained matrix. Field-width ~20 mm.

sent crystals equilibrated with the melt; they are quench products. Plagioclase forms bundles of skeletal crystals, intergrown with the olivines. The plagioclases are slightly strained, clouded and contain prominent fluid inclusions. The interstices are filled with brown clinopyroxene, ilmenite, Ti-magnetite and Cr-spinel. Composite blebs of pyrrhotite and chalcopyrite also occur. The complete lack of intratelluric phenocrysts suggests that this sample represents a fast-crystallized picritic melt.

4.c. Sample M9

M9 is an example of the rare Group 3 picritic intrusions. It contains ~60 ± 5% olivine phenocrysts (macrocrysts) and ~3% spinel phenocrysts. The olivines show a large, continuous size range < 0.5–7 mm and the spinels vary from 0.2–1 mm. The olivines are mainly subhedral equant (polyhedral and granular: Donaldson, 1976) whereas a few are of hopper type. Some contain deformation lamellae and some show marginal hydrothermal alteration of the olivines to serpentine, chlorite and magnetite (Haggerty & Baker, 1967).

The dyke matrix contains sheaths of sub-parallel and partially radiating olivine and pyroxene, with plagioclase crystals up to 15 mm long and often hollow-cored and H-shaped (Fig. 3a). Olivine, clinopyroxene, ilmenite and magnetite occur interstitially.

The olivine phenocrysts are divisible into two, apparently discrete, populations referred to as Types A and B (Fig. 3b). Those of Type A have a brownish coloration in thin-section due to finely exsolved trails of Fe-oxides, probably resulting from high temperature oxidation (Haggerty & Baker, 1967), which confers the dark coloration to the dyke in outcrop. The cores of the Type A phenocrysts are very magnesian, ranging up to almost $Fo_{93.0}$, with some normal zoning to colourless rims of $Fo_{87.1}$. Type B phenocrysts, in contrast, are colourless and are systematically less magnesian ($Fo_{90.2}$ zoned to $Fo_{86.2}$). The two types also differ significantly in their minor element contents, the Type A olivines being significantly richer in Cr, Ca and Ni but poorer in Mn than the Type B olivines.

The observation that Type B olivine surrounds some of the Type A olivines, in conjunction with the difference in forsterite content, implies that the Type A olivines crystallized in a higher temperature environment and that Type B crystallized subsequently. The Type B crystals are more variable in appearance being predominantly patchy with clear, cloudy and, locally, 'brown' areas. Although the Type B phenocrysts are generally distinguishable from Type A they are themselves a heterogeneous population with compositions

https://doi.org/10.1017/S0016756802006684 Published online by Cambridge University Press

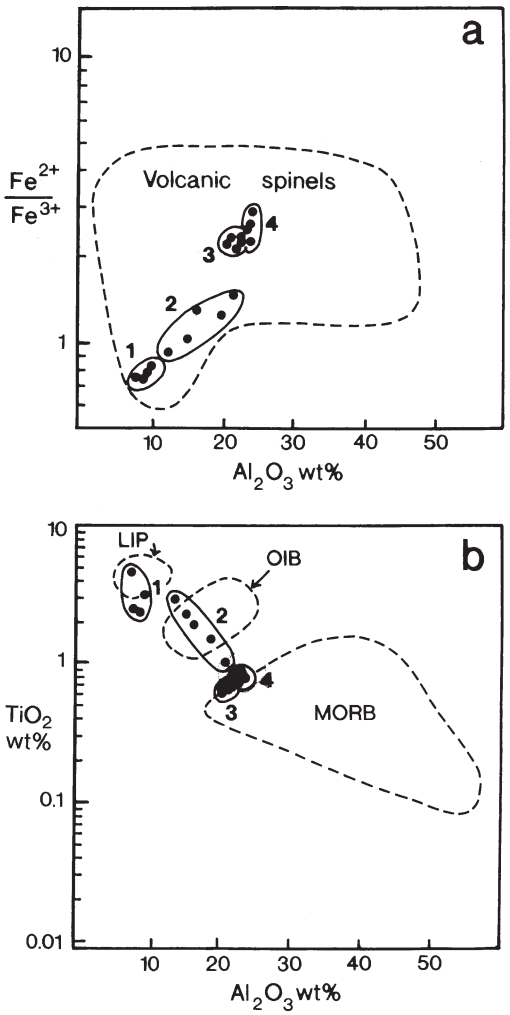

Figure 4. (a) Plot of Al_2O_3 vs. Fe^{2+}/Fe^{3+} for Cr-spinels from the picritic dykes and for magnetites from the matrix of B65. 'Field for volcanic spinels' after Kamanetsky, Crawford & Meffre, 2001. (b) Plot of Al_2O_3 vs. TiO_2 for spinels from the picritic dykes. Fields 1, 2, 3 and 4 are those of Cr-spinels in samples B65, B62/2, M9 Type A olivine phenocrysts and in Type B olivine phenocrysts respectively. Other fields, enclosed by dashed lines, are from Kamenetsky, Crawford & Meffre, 2001. LIP = Large Igneous Provinces.

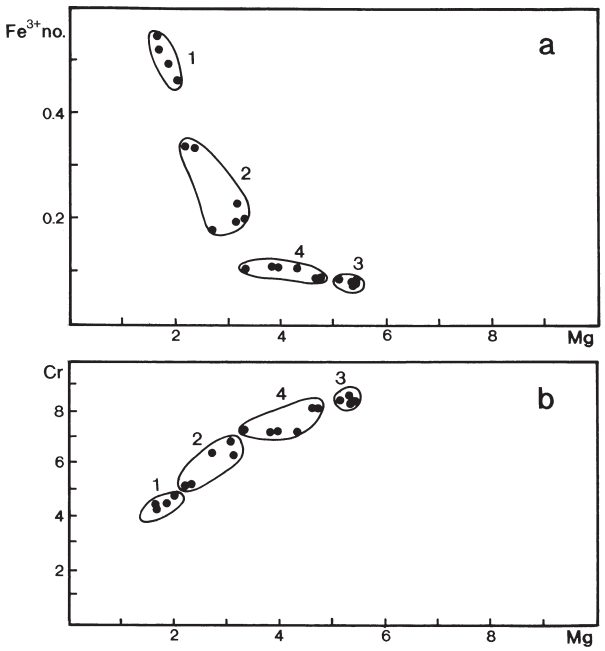

Figure 5. (a) Plot of Fe^{3+} no. vs. Mg for chrome spinels from the picrites (where Fe^{3+} no. = $Fe^{3+}/(Fe^{3+} + Al + Cr)$. (b) Plot of Cr vs. Mg for the chrome spinels. Fields 1, 2, 3 and 4 as in Figure 4.

differing from crystal to crystal, for example, some phenocrysts are consistently $Fo_{86–87}$, others $Fo_{87–88}$ or $Fo_{89–90}$. Forty-four analyses from the cores of twenty-five different crystals gave a mean composition of $Fo_{88.2}$. No difference was found between the clear, cloudy or brown areas of Type B phenocrysts nor any sign of marginal zoning. Compositions of $Fo_{84.4–83.0}$ were noted from the groundmass olivines of M9.

Pargasitic rims to clinopyroxenes in M9 may have formed by late-stage reaction with residual melts (Kent, 1995). The spinels are Al–Cr picotites (Table 1), whose cores were regarded by McClurg (J. McClurg, unpub. Ph.D. thesis, Univ. Edinburgh, 1982) as representing liquidus compositions protected from reaction with later residual melts by the enclosing olivines. The original high temperature chemistry of the spinels in M9 (as well as in B62/2) is believed to have been preserved by quenching (J. McClurg, unpub. Ph.D. thesis, Univ. Edinburgh, 1982).

The compositional differences in the two populations of olivine phenocrysts are reflected in compositional differences in their spinel inclusions (Fig. 4). Those in Type A olivines have slightly lower Fe^{2+}/Fe^{3+} ratios (calculated according to Droop, 1987) than those in Type B, suggesting that the Type A olivines (and their included spinels) experienced an oxidation event that pre-dated crystallization of the Type B olivines. The 'Type A' spinels have slightly lower TiO_2 and Al_2O_3 but higher Cr_2O_3 than those in the younger Type B olivines. The spinel inclusions in Type A olivine phenocrysts also differ from those in Type B olivines in having more Mg, Ni and Zn but less Fe, Mn and V, supporting the contention that Type A olivines and their spinel inclusions were derived from a higher-temperature, more primitive stage of the magmatic evolution.

Chrome spinels from the three samples fall into compositionally distinct fields as shown in Figures 4 and 5. These show a positive correlation between Mg and Cr and a negative correlation between Mg and Fe^{3+} no. where the Fe^{3+} no. = $Fe^{3+}/(Fe^{3+} + Al + Cr)$. Spinels in M9 have the highest Mg and those of B65, the lowest. The spinels from the three dykes display a roughly continuous trend of increasing TiO_2 with falling Al_2O_3 (Fig. 4b), transgressing the compositional fields delineated by Kamanetsky, Crawford & Meffre (2001) for Cr spinels from Large Igneous

https://doi.org/10.1017/S0016756802006684 Published online by Cambridge University Press

Table 1. Representative analyses of olivines and oxides in Rum picrites

	Olivines				Cr- spinels				Magnetite	Ilmenite
	1	**2**	**3**	**4**	**5**	**6**	**7**	**8**	**9**	**10**
V_2O_5	n.d.	n.d.	n.d.	n.d.	0.10	0.19	0.23	0.35	1.12	0.60
SiO_2	40.83	40.27	40.17	38.09	0.22	0.18	0.12	0.11	0.14	0.10
TiO_2	n.d.	n.d.	n.d.	n.d.	0.72	0.86	1.82	2.83	3.07	52.69
Al_2O_3	0.14	0.10	0.13	0.07	20.61	23.28	16.34	9.82	1.75	0.09
Cr_2O_3	0.17	0.08	0.06	0.03	44.52	37.29	32.99	22.55	0.16	0.21
Fe_2O_3	n.d.	n.d.	n.d.	n.d.	6.32	8.80	17.72	33.60	63.75	0.69
FeO	7.07	11.03	13.44	21.95	12.27	17.27	21.26	24.97	27.98	40.89
MnO	0.12	0.18	0.22	0.46	0.29	0.34	0.40	0.42	0.19	0.76
MgO	50.94	47.93	45.82	38.96	14.50	11.53	7.98	4.84	2.00	4.05
NiO	0.43	0.36	0.34	0.15	0.26	0.22	0.18	0.16	0.17	0.04
ZnO	n.d.	n.d.	n.d.	n.d.	0.28	0.21	0.00	0.00	0.00	0.00
CaO	0.24	0.16	0.49	0.03	n.d.	n.d.	n.d.	n.d.	n.d.	n.d.
Total	99.94	100.11	100.67	99.74	100.09	100.17	99.05	99.65	100.32	100.12
	Formulae recast to 4 oxygens				Formulae recast to 24 cations and 32 oxygens					Formula recast to 4 cations and 6 oxygens
V^{5+}	n.d.	n.d.	n.d.	n.d.	0.016	0.031	0.040	0.065	0.222	0.019
Si^{4+}	0.992	0.994	0.997	0.994	0.054	0.045	0.032	0.031	0.042	0.005
Ti^{4+}	n.d.	n.d.	n.d.	n.d.	0.133	0.160	0.363	0.596	0.692	1.937
Al^{3+}	0.004	0.003	0.004	0.002	5.973	6.807	5.109	3.240	0.619	0.005
Cr^{3+}	0.003	0.001	0.001	0.001	8.654	7.313	6.918	4.991	0.038	0.008
Fe^{3+}	n.d.	n.d.	n.d.	n.d.	1.170	1.643	3.537	7.077	14.387	0.025
Fe^{2+}	0.143	0.227	0.279	0.479	2.523	3.582	4.716	5.844	7.016	1.672
Mn^{2+}	0.003	0.004	0.005	0.010	0.060	0.071	0.090	0.100	0.048	0.031
Mg^{2+}	1.845	1.763	1.695	1.515	5.315	4.264	3.156	2.020	0.894	0.295
Ni^{2+}	0.009	0.007	0.007	0.003	0.051	0.044	0.038	0.036	0.041	0.002
Zn^{2+}	n.d.	n.d.	n.d.	n.d.	0.051	0.038	0.000	0.000	0.000	0.000
Ca^{2+}	0.006	0.004	0.013	0.001	n.d.	n.d.	n.d.	n.d.	n.d.	n.d.
Cation sum	3.005	3.004	3.001	3.005	24.000	24.000	24.000	24.000	24.000	4.000
Mg.100/(Fe^{2+}+Mg)	92.8	88.6	85.9	76.0	67.8	54.3	40.1	25.7	11.3	15.0

1 – Core, Type A phenocryst, M9; **2** – Core, Type B phenocryst, M9; **3** – Core, phenocryst, B62/2; **4** – Core, phenocryst, B65; **5** – Inclusion in Type A olivine, M9; **6** – Inclusion in Type B olivine, M9; **7** – Inclusion in olivine phenocryst, B62/2; **8** – Inclusion in olivine phenocryst, B65; **9** – Magnetite intergrown with ilmenite, B65; **10** – Ilmenite intergrown with magnetite, B65

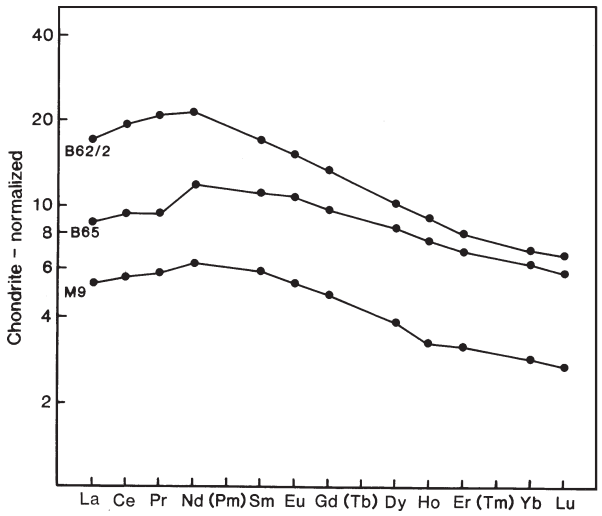

Figure 6. Chondrite-normalized REE patterns for the three picrite samples. Normalizing values after Thompson (1982).

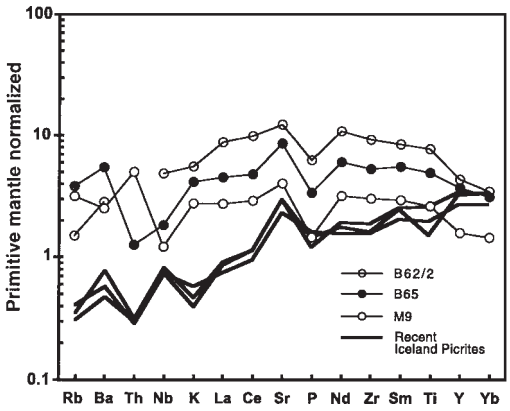

Figure 7. Primitive mantle-normalized incompatible element patterns for the three picrite samples. Normalizing values after McDonough & Sun (1995). Recent Iceland picrite data from Skovgaard *et al*. (2001).

Provinces (LIP), Ocean Island Basalt (OIB) and Mid-Ocean Ridge Basalt (MORB) environments.

Whilst the B62/2 spinels have distinctly higher V, Ti, Fe, Mn and Zn and lower Al, Cr, Mg and Ni than those in the M9 olivine phenocrysts, these compositional characteristics are still more extreme in the B65 spinels. The picritic dyke spinels show continuous gradation to Fe^{3+}-rich compositions with roughly constant Al/Cr ratio, and spinel appears to have been a stable phase throughout the crystallization history.

The dyke spinels are relatively Cr-poor in comparison to those from the layered cumulates of the island, probably due to their crystallization at higher pressures where the Mg–Al couple is stable, followed by higher f_{O2}.

Representative analyses of olivines and spinels from the three samples are presented in Table 1.

5. Whole-rock compositions

Major and trace element analyses are presented in Table 2. B65 and B62/2 are regarded as reflecting melt compositions with little or no accumulative olivine. They have MgO contents of 12.4 and 14 wt%, Ni contents of B62/2 and B65 are 353 and 404 ppm, respectively. The relatively high Cu contents of these two samples (164 and 153 ppm) accord with the observations on modal sulphides. In contrast, M9 is inferred to represent a mush of non-equilibrated olivine (and spinel) crystals within a highly magnesian melt.

The Zr/Nb ratios of the three samples are in the range 30–47 whereas Ce/Y values are notably low, 0.5–0.9. La/Nb values lie from 1.7 to 2.5 and Ba/Nb values lie between 6 and 30. Chondrite-normalized REE patterns (Fig. 6) show convex-upward forms with negative slopes from Nd to Lu. Primitive mantle-normalized plots for the incompatible elements indicate negative anomalies for Nb (relative to La) and for P (relative to Sr and Nd; Fig. 7) whereas Sr shows positive anomalies (relative to Ce and Nd). Comparison with trace element spectra for recent Iceland picrites reveals similarities in that the latter also possess positive anomalies for Sr and negative anomalies for P.

6. Oxygen isotopes

Replicate oxygen isotope ratio compositions were determined for the three whole-rock samples at the Scottish Universities Research Reactor Centre (SURRC), East Kilbride. Oxygen was released from *c*. 10 mg of sample powder (approx. 200 mesh) by the conventional fluorination method of Clayton & Mayeda (1963) as modified by Borthwick & Harmon (1982) for operation with chlorine trifluoride. The released gas was purified cryogenically and converted to CO_2 over hot platinized graphite. Isotopic essay of the CO_2 was performed on a dual-inlet triple collector mass spectrometer with reference gas calibrated against international carbonate and water standards. For NBS 28 quartz this procedure gives $\delta^{18}O$ (V-SMOW) = 9.6‰ with a one σ standard deviation of ± 0.1‰. For whole-rock powders, precision is probably around 0.2‰.

$\delta^{18}O$ values for B65 and B62/2 lie within the normal range for mantle-derived magmatic rocks; duplicate values for the former being +5.5 and 5.6‰ and +6.0 and 6.3‰ respectively. Only two out of forty-one analysed samples from the layered cumulate suite have comparable values, all others having values between –4.8 and +4.7‰ indicative of extensive subsolidus hydrothermal interaction with low $\delta^{18}O$ fluids (Emeleus, 1997, and references therein). However, the value of $+1.2 \pm 0.2$‰ obtained from M9 might imply that this dyke experienced a high-temperature hydrothermal alteration by a low $\delta^{18}O$ fluid.

https://doi.org/10.1017/S0016756802006684 Published online by Cambridge University Press

Table 2. Whole-rock analyses of picrite dykes, Rum

	B62/2	B65	M9
Major elements (wt %)			
SiO_2	45.76	46.66	41.87
Al_2O_3	13.58	15.18	5.86
Fe_2O_3*	12.38	11.22	10.7
MgO	12.42	14.01	34.14
CaO	11.25	10.49	4.5
Na_2O	2.23	2.17	0.79
K_2O	0.16	0.12	0.08
TiO_2	1.56	0.99	0.53
MnO	0.19	0.16	0.16
P_2O_5	0.13	0.07	0.03
L.o.I	0.51		1.36
Total	100.16	101.08	100.02
Trace elements (ppm)			
Ni	353	404	1990
Cr	720	798	2137
V	339	250	121
Sc	33	25	11
Cu	164	153	59
Zn	78	70	60
Rb	0.9	2.3	1.9
Ba	18.8	36	16.6
Sr	244	171	80
Th	(b.d.)	0.1	0.4
Pb	1.5	1.8	0.9
Zr	97	56	32
Nb	3.2	1.2	0.8
Y	18.8	16	6.8
Rare-earth elements			
La	5.67	2.94	1.78
Ce	16.56	8.04	4.87
Pr	2.57	1.16	0.71
Nd	13.54	7.56	3.99
Sm	3.44	2.26	1.2
Eu	1.19	0.84	0.41
Gd	3.69	2.72	1.36
Dy	3.49	2.86	1.32
Ho	0.69	0.58	0.25
Er	1.81	1.57	0.72
Yb	1.53	1.38	0.64
Lu	0.23	0.2	0.09
La/Yb	3.71	2.13	2.78
Zr/Nb	30.3	46.7	40
Ce/Y	0.88	0.5	0.71
La/Nb	1.77	2.45	2.2
Ba/Nb	5.9	30	20.8
Sr anomalies (Sr/Sr*)	1.18	1.58	1.32

Fe_2O_3* total iron as Fe_2O_3; Sr* = $(Ce_N \times Nd_N)0.5$; normalization to primitive mantle (McDonough & Sun, 1995).

7. Radiogenic isotopes

All three samples were analysed for Sr, Nd, Pb and Os isotopes. Sr and Nd analyses were carried out on whole-rock samples at the Scottish Universities Research Reactor Centre. Sr isotopes were analysed on a VG 54E thermal ionization mass spectrometer. $^{87}Sr/^{86}Sr$ was corrected for mass fractionation using $^{86}Sr/^{88}Sr = 0.1194$. Repeat analysis of NBS987 Sr standard gave $^{87}Sr/^{86}Sr = 0.710219 \pm 26$ (2 s.d., n = 9), and all data were normalized to a value of $^{87}Sr/^{86}Sr = 0.710243$ for this standard. Nd data were obtained

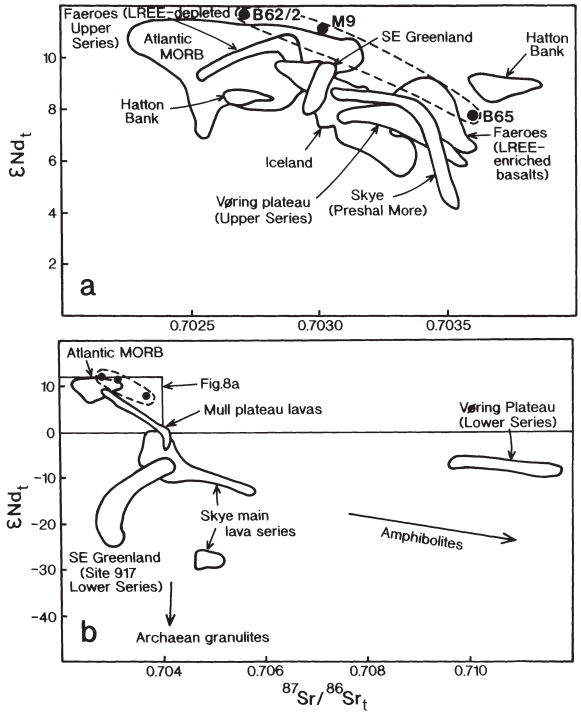

Figure 8. $^{87}Sr/^{86}Sr$ vs. ε_{Nd} diagram. After Saunders *et al.* 1997.

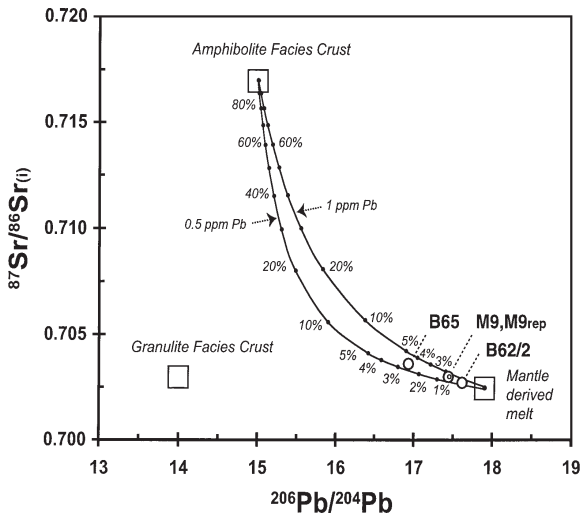

Figure 9. $^{87}Sr/^{86}Sr$ vs. $^{206}Pb/^{204}Pb$ diagram. Errors are smaller than the size of the symbols. Binary mixing modelling suggests between ~0.54% and ~4.8% assimilation of amphibolite-facies crust. Mixing parameters for a primary mantle-derived picritic melt ([Pb] = 0.5 and 1 ppm respectively; $^{206}Pb/^{204}Pb$ = 17.9 (Thirlwall, 1995; Chauvel & Hémond, 2000); $^{87}Sr/^{86}Sr = 0.7024$, [Sr] = 115 ppm) and for amphibolite- and granulite-facies crust ($^{206}Pb/^{204}Pb$ = 15.0, [Pb] = 10 and 12 ppm respectively, $^{87}Sr/^{86}Sr = 0.7170$, [Sr] = 287 ppm (Dickin, 1981; Palacz, 1985). The required mixing proportions with crust for a mantle-derived melt containing 0.5 and 1 ppm Pb respectively; B65 (2.5% and 3.8%), M9 (0.9% and 1.8%) and B62/2 (0.4% and 0.5%).

using a VG Sector 54-30 thermal ionization mass spectrometer in multi-dynamic mode. $^{143}Nd/^{144}Nd$ was corrected for mass fractionation using $^{146}Nd/^{144}Nd = 0.7129$. During the course of this study the SURRC

https://doi.org/10.1017/S0016756802006684 Published online by Cambridge University Press

Table 3. Oxygen-, Sr-, Nd-, Pb- and Os-isotope ratios for Rum picrites

Sample Age (Ma)	B62/2 60.5	B65 60.5	M9 60.5	$M9_{rep}$
$\delta^{18}O_{SMOW}$ (‰)	6.0	5.5	1.0	
$\delta^{18}O_{SMOW}$ (‰)$_{rep}$	6.3	5.6	1.3	
$^{87}Sr/^{86}Sr$	0.702714±13	0.703636±12	0.703073±12	
$^{87}Rb/^{86}Sr$	0.011	0.039	0.069	
$^{87}Sr/^{86}Sr_{(i)}$	0.702705	0.703603	0.703014	
Sm (ppm)	3.44	2.26	1.20	
Nd (ppm)	13.54	7.56	3.99	
$^{143}Nd/^{144}Nd$	0.513225±4	0.513022±7	0.513199±6	
ε_{Nd}	11.5	7.5	10.9	
$^{147}Sm/^{144}Nd$	0.1539	0.1811	0.1822	
$^{143}Nd/^{144}Nd_{(i)}$	0.513164	0.512950	0.513127	
$\varepsilon_{Nd\ (i)}$	10.4	6.1	9.6	
$^{206}Pb/^{204}Pb$	17.621	16.925	17.453	17.441
2 sd. error	0.026	0.013	0.014	0.026
$^{207}Pb/^{204}Pb$	15.332	15.186	15.302	15.288
2 sd. error	0.027	0.014	0.013	0.027
$^{208}Pb/^{204}Pb$	37.062	37.098	37.459	37.425
2 sd. error	0.026	0.013	0.013	0.027
Re (ppb)	1.97	1.34	1.28	
Os (ppb)	1.42±6	0.38±6	1.73±7	
$^{187}Os/^{188}Os$	0.1452±9	0.1515±9	0.1321±4	0.1319±8
$^{187}Re/^{188}Os$	6.68	17.18	3.56	
$^{187}Os/^{188}Os_{(i)}$	0.1385	0.1343	0.1285	0.1284

rep - replicate analysis

internal JM Nd laboratory standard gave $^{143}Nd/^{144}Nd = 0.511501 \pm 12$ (2 s.d.).

Pb and Os isotope analyses were carried out at the University of Copenhagen. After leaching in 6N HCl at 190 °C for 1 hour, Pb was separated using standard ion exchange techniques and isotope ratios were analysed on a VG-Sector 54 mass spectrometer. Pb was conventionally separated in 0.5 ml glass columns charged with anion exchange resin AG1-X8 (100–200 mesh) using a standard HBr–HCl–HNO_3 elution recipe, followed by a clean-up on 300 µ Teflon columns (Frei & Rosing, 2001). After loading Pb on Re filaments with silica gel and H_3PO_4 the samples were analysed on a Fisons VG Sector 54-IT (T-IMS) in static multi-collector mode. The total procedural Pb blank amounted to < 90 pg during the analytical session, which is considered insignificant with respect to contamination of the sample leads in any of the three samples. Fractionation for Pb was controlled by repetitive analyses of SRM-981 standard (values of Todt *et al.* 1993) as routinely analysed in this laboratory. SRM-981 analyses during the analytical session of the Rum samples yielded 16.892 ± 0.0078 for $^{206}Pb/^{204}Pb$, 0.91366 ± 0.0015 for $^{207}Pb/^{206}Pb$ and 2.1620 ± 0.0015 for $^{208}Pb/^{206}Pb$ (all 2σ of the population). The fractionation correction amounted to 0.07 % a.m.u.

Samples were prepared for Os isotopic analysis by the carius tube digestion techniques (Shirey & Walker, 1998; Nägler & Frei, 2001) and were analysed by N-TIMS as single multiplier analyses. Os concentrations were determined by isotope dilution analysis. Total procedural blanks for Os were less than 0.7 pg. Blank corrections ranged from 0.04 % to 1.2 % on the $^{187}Os/^{188}Os$ ratios. Within-run uncertainties on $^{187}Os/^{188}Os$ ranged from 0.2 % to 0.8 % (2σ standard error of the mean). A full procedural replicate analysis agreed within 0.09 % on the $^{187}Os/^{188}Os$ ratios. Isotope data and Sr, Nd, Pb, Os and Re concentrations are reported in Table 3 together with analytical details and errors.

The results are variable and range from Atlantic MORB values ($^{87}Sr/^{86}Sr$ 0.7022–0.7032; $^{143}Nd/^{144}Nd$ 0.5130–0.5132) (Saunders *et al.* 1997) for samples M9 and B62/2, to more radiogenic Sr and less radiogenic Nd values for sample B65 (Fig. 8; Table 3). The slight variation in Sr and Nd between B62/2 and M9 may relate either to very minor amounts of crustal contamination or to source differences between those for the B62/2 dyke cutting the Eastern Layered Series and M9 cutting the Western Layered Series. B62/2 and M9 have higher $^{206}Pb/^{204}Pb$, $^{207}Pb/^{204}Pb$ and $^{208}Pb/^{204}Pb$ ratios than B65 although all are lower than the range of Atlantic MORB (Thirlwall, Upton & Jenkins, 1994; Chauvel & Hémond, 2000). The samples all have less radiogenic lead values than those reported by Palacz (1985) for the Eastern Layered Series cumulates but overlap the range determined for the Skye Main Lava Series (Dickin, 1981). Each of the three samples appears to have been affected by some form of mixing or contamination with a source more radiogenic in Sr isotopes than MORB.

The Pb isotope ratios extend from those of a

https://doi.org/10.1017/S0016756802006684 Published online by Cambridge University Press

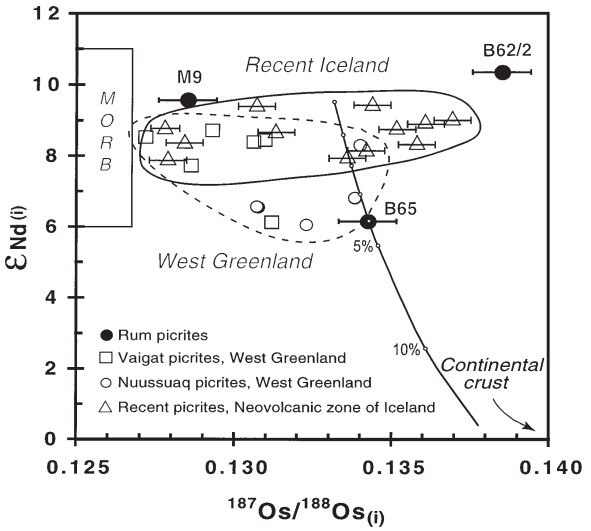

Figure 10. $^{187}Os/^{188}Os$ vs. ε_{Nd} data for West Greenland picrites from Schaefer, Parkinson & Hawkesworth (2000). Shaded field for the MORB reservoir is represented by analyses of abyssal peridotites (Roy-Barmann & Allègre, 1994; Snow & Reisberg, 1995; Parkinson Hawkesworth & Cohen, 1998). Field for recent Iceland picrites from Skovgaard *et al.* (2001) and A. C. Skovgaard (unpub. data). End-member parameters for mixing line: average continental crust; (Os = 0.01 ppb $^{187}Os/^{188}Os$ = 2.5, Nd = 20 ppm, ε_{Nd} = –25.0, Rum primary melt (Os = 1 ppb, $^{187}Os/^{188}Os$ = 0.1332, Nd = 8 ppm, ε_{Nd} = 9.5. Estimates of the end-member parameters are based on Palacz (1985), Esser & Turekian (1993), Schaefer, Parkinson & Hawkesworth (2000) and Peuker-Ehrenbrink & Jahn (2001).

mantle-derived melt, similar to depleted Icelandic basalts, towards values for amphibolite- and granulite-facies crust (Dickin, 1981), as shown in the covariance of $^{87}Sr/^{86}Sr$ vs. $^{206}Pb/^{204}Pb$ (Fig. 9). The distinctly higher $^{87}Sr/^{86}Sr$ and lower $^{143}Nd/^{144}Nd$, $^{206}Pb/^{204}Pb$, $^{207}Pb/^{204}Pb$ and $^{208}Pb/^{204}Pb$ ratios of B65 are likely to reflect greater interaction of this melt with upper crustal rocks.

Comparison of the Sr and Nd data from the Eastern Layered Series (Palacz, 1985) with those for the picritic dykes shows B62/2 to be more primitive than all samples previously measured, whilst B65 is comparable to the troctolites of Eastern Layered Series Units 13 and 14.

The samples have high Os concentrations (0.4–1.7 ppb) and markedly more radiogenic $^{187}Os/^{188}Os$ isotope ratios than the MORB reservoir (Fig. 10), taking into account that the high Re/Os ratios necessitate a considerable age correction given the age of the Rum picrites (Table 3). Os isotope values are slightly suprachondritic with $^{187}Os/^{188}Os_{(i)}$ varying from 0.1284 to 0.1385, corresponding to $\gamma Os_{(60.5Ma)}$=1.0–8.9. The Os isotope and ε_{Nd} variation in the Rum picrites partly overlaps that shown by recent Iceland picrites and early Tertiary West Greenland picrites (Schaefer, Parkinson & Hawkesworth, 2000; Skovgaard *et al.* 2001), (Fig. 10). Sample B62/2 has MORB-like ε_{Nd} but an Os isotope composition that is more radiogenic than recent Icelandic picrites (Fig. 10).

8. Discussion

8.a. Temperature, pressure and MgO content of the primitive melt

There is general consensus amongst previous workers that the magmas involved in the generation of the Rum basic–ultrabasic complex were high-temperature melts with magnesium contents > 13 %, that is, picrites (LeBas, 2000). These melts were also mildly alkalic (J. McClurg, unpub. Ph.D. thesis, Univ. Edinburgh, 1982; Faithfull, 1985; Volker & Upton, 1990).

Of the three samples, M9 is of special interest in containing a bimodal population of olivine phenocrysts (or macrocrysts), the earliest of which have compositions approximating to Fo_{93}. Thompson & Gibson (2000) commented on the rarity of such extreme olivine compositions in Phanerozoic magmatic rocks; examples are known sparingly from picrites of Baffin Island (Francis, 1985), West Greenland (Larsen & Pedersen, 2000), Gorgona (Révillon *et al.* 2000) and Namibia (Thompson & Gibson, 2000) as well as from meimechites in Siberia (Arndt, Lehnert & Vasil'ev, 1995).

The closest parallels to M9 appear to be some of the Horingbaai dykes of Namibia which also carry bimodal populations of forsteritic olivine (up to $Fo_{93.3}$). Thompson & Gibson (2000) concluded that most magnesian olivines crystallized from unerupted komatiitic melts whose high densities caused them to be retained beneath the crust. These olivines were subsequently entrained by less magnesian melts. A comparable evolution is envisaged for the Type A olivines of M9, which having already been subjected to a high temperature oxidation event, were entrained by a melt containing a population of olivine phenocrysts ranging from $Fo_{90.2}$ to $Fo_{86.2}$. In view of the rapidity with which Fe–Mg equilibration occurs at magmatic temperatures, this disequilibrated ensemble must then have rapidly reached shallow crustal levels where, as a small volume of magma intruded into relatively cold country rocks, it also cooled fast. The Type A olivines have CaO (up to 0.46 wt %) and Cr_2O_3 (up to 0.17 wt %) contents well above those typical for mantle peridotites, thus negating the possibility that they represent mantle-derived xenocrysts (cf. Thompson & Gibson, 2000). The Cr contents are also much greater than those for most olivines in magnesian basalts (< 0.02 Cr_2O_3 wt %) and signify unusually high temperatures (Li, O'Neill & Seifert, 1995).

McClurg (unpub. Ph.D. thesis, Univ. Edinburgh, 1982) concluded that the Type A olivines crystallized at depth from a high-Mg liquid in equilibrium with mantle olivines, stating that the composition of their

https://doi.org/10.1017/S0016756802006684 Published online by Cambridge University Press

spinel inclusions also denotes high-pressure origin. Kent (1995) corroborated this, observing that the M9 spinel inclusions resemble those stable at 1.0 Gpa in anhydrous partial melts of spinel lherzolite and pyrolite compositions, suggesting their crystallization at near-Moho depths of 25–30 km. This inference of sub-crustal crystallization accords with Thompson & Gibson's deduction of sub-crustal crystallization of the Horingbaai forsterites.

Thompson & Gibson (2000) proposed that the most magnesian Horingbaai olivines crystallized from a melt with ~24 wt% MgO whilst for the Siberian meimechites (Arndt, Lehnert & Vasil'ev, 1995) melts with 25 to 29 wt% MgO have been proposed. However, it is not possible to reach any precise conclusion for the MgO content of the Type A parent melt in view of several uncertainties: the coefficient for Fe^{2+}–Mg partitioning between olivine and liquid is pressure dependent (Ulmer, 1989) and the pressure of crystallization in the present instance is indeterminate. Since the possibility of some equilibration between olivines and spinels and/or oxidation (increasing the Fo content of the former) cannot be discounted, ~Fo_{93} may be too high a value for the original (magmatic) composition of M9 macrocrysts. Work in progress on the Western Layered Series (L. Worrell, pers. comm.) suggests that Fo values may have been elevated by ~1% giving us Fo_{92} as the possible maximum forsterite content. The most magnesian olivines in Hawaii are $Fo_{91.3}$, corresponding to a melt with 17 wt% MgO (Garcia, Hulsebosch & Rhodes, 1995) whilst the Gorgona picrites have megacryst olivine cores ranging up to Fo_{94} crystallized from melts with 20–25 wt% MgO (Révillon *et al.* 2000). It is likely that the Type A macrocrysts grew at slightly higher temperatures from more magnesian melts than those of Hawaii. McClurg's (unpub. Ph.D. thesis, Univ. Edinburgh, 1982) selection of the most primitive melt composition was based on the most magnesian of the aphyric picrites (B65) and the quenched matrix of M9 which she calculated as having 20.5 wt% MgO. Since at least some of the olivine macrocrysts in M9 must have grown at the expense of the surrounding melt, she suggested that 20.5 wt% may represent a minimum value for the parent melt. Kent (1995) considered that the M9 olivines should have been in equilibrium with a dry melt containing 18–20 wt% MgO at 1420–1460 °C, calculated after Ford *et al.* (1983) on the assumption that the olivine compositions have not been modified by secondary oxidation or reaction with spinel. Although the presence of accessory amphiboles and biotites indicates that melting cannot have been 'dry', we are prepared to accept 18–20 wt% as the best estimate and view values > 20%, such as proposed for Horingbaai (Thompson & Gibson, 2000), as improbable in view of the exceptional degrees of melting (and hence temperatures) implied.

The Fe^{2+}/Fe^{3+} ratio of the melt, calculated by the method of Maurel & Maurel (1982), was used to deduce the oxygen fugacity of the melt (Danyushevsky & Sobolev, 1996). This gave a $\log^{10}$ oxygen fugacity of –6.0, close to the QFM buffer.

The crust beneath Rum is likely to consist largely of relatively dense granulite-facies rocks (Upton, Aspen & Hinton, 2001) in which the picrite magmas would have been nearly neutrally bouyant. Since the presence of volatiles in the magmas would have aided their ascent, no great over-pressures need be postulated for their eruption to near-surface levels.

The Long Loch Fault is assumed to have overlain a zone of weakness that facilitated magma ascent. The precise nature of the displacement along the Long Loch Fault remains obscure but it probably had an early Tertiary right-lateral component (Emeleus, 1997) and possessed some dilational component in the vicinity of Rum. Furthermore, such a proto-Long Loch fault may have had an influence from surface levels to the base of the lithosphere, permitting decompression of the underlying plume-head peridotite whilst simultaneously providing a conduit for the picritic melts so generated. It may be further speculated that the pulsatory build-up of the Rum layered cumulate series itself reflected repetitive movements along the fault.

8.b. Melting conditions

The relatively high Nd/Lu ratios of the samples (38–59) suggest an origin in garnet-facies mantle source rocks in which garnet remained as a refractory residual. The low contents of Y and Sc also point to the genesis of these melts in garnet-facies peridotites, with the melt fraction being small enough for garnet to remain in the refractory residue. Accordingly, the data do not support the contention by Butcher *et al.* (1999) that the Rum parental magmas were linked to a 'high-degree of melting', although the association with mantle plume activity remains highly probable. Conversely, the dyke data presented here corroborate the findings of Henderson & Gijbels (1976), who concluded that the parent magmas for the layered cumulates on Rum were enriched in LREE relative to HREE and were produced from small amounts of partial melting of mantle source rocks. Henderson & Gijbels also noted from REE study of the Eastern Layered Series cumulates that the source region was relatively homogeneous and did not experience significant change in degree of partial melting during formation of the layered series.

The REEs were used to derive an estimate for the degree and depth of melting, assuming continuous removal and collection of fractional melts and using distribution coefficients and depleted elemental abundances from McKenzie & O'Nions (1991). Conclusions from modelling these data, and the major element data, suggest that the parental magma was a ~6–7% mantle melt, with melting occurring between

https://doi.org/10.1017/S0016756802006684 Published online by Cambridge University Press

110 and 85 km depth, and thus straddling the garnet–spinel transition. The slopes of the REE patterns are not steep enough for all melting to be in the garnet zone, although most of the melting would have occurred in the presence of garnet. If adiabatic upwelling is assumed, the modelling leads to an estimated mantle potential temperature of ~1550 °C (about 250 °C above ambient temperature). The major assumption made here is that the melting occurred under dry conditions, although this is clearly an oversimplification in view of the petrography. Melting under hydrous conditions would require lower mantle potential temperatures.

It has been suggested that garnet-imposed geochemical signatures may not be due to initiation of melting within the garnet lherzolite facies mantle but might derive from melting at shallower depths within heterogeneous spinel lherzolite sources containing intercalated layers of garnet pyroxenite (Hirschmann & Stolper, 1996; Klemme & O'Neill, 2000). This possibility, however, apppears to be negated by Lu–Hf isotopic systematics of garnet pyroxenites (Blichert-Toft, Albarède & Kornprobst, 1999).

8.c. Crustal contamination of the picritic magmas

The low concentrations of incompatible elements would have made the picritic magmas highly susceptible to contamination by continental crustal lithologies in which there are high concentrations of incompatible elements.

In order to assess the possible effect of contamination on the Sr, Nd and Pb isotopic compositions of the Rum picrites, we have assumed that the primary mantle-derived melt was similar in $^{87}Sr/^{86}Sr$, $^{143}Nd/^{144}Nd$, $^{206}Pb/^{204}Pb$ and $^{187}Os/^{188}Os$ isotopic composition to recent, depleted picrites from Iceland, which only differ significantly from North Atlantic MORB in their Os isotope characteristics (Chauvel & Hémond, 2000). The isotopic composition of the local amphibolite-facies crust is taken from Dickin (1981) and Palacz (1985). Mass balance calculations of Sr and Pb isotope systematics show that B65 can be modelled by approximately 2.5–4.8% contamination with amphibolite-facies crust (Fig. 9), with Pb contents of mantle-derived melt of 0.5 and 1 ppm respectively. Much smaller degrees of crustal contamination (< 1.8%) affected samples B62/2 (0.5% and 1%) and M9 (0.9% and 1.8%). This study thus accords with the deduction by Dickin (1981) that Pb isotope ratios in the British Tertiary Volcanic Province provide insights into the nature of the contaminant but not the mantle source. On the basis of Pb and Sr isotopic systematics, it is most likely that the local crustal contaminant was amphibolite-facies rather than granulite-facies crust.

The Os isotope compositions provide better constraints on the mantle source of the Rum picrites as their high Os concentrations relative to crustal values (50 : 1) (e.g. Esser & Turekian, 1993) makes them less susceptible to contamination. The effect of crustal contamination on the $^{187}Os/^{188}Os$ isotopic ratio is illustrated for sample B65 in Figure 10. Here a hypothetical mantle-derived picritic melt with ε_{Nd} and $^{187}Os/^{188}Os$ isotope characteristics similar to those of recent Icelandic picrites, is relatively displaced to lower values, whereas only a minor effect is seen on the $^{187}Os/^{188}Os$ ratio.

That crustal contamination was the cause of the variability in $^{187}Os/^{188}Os$ ratios is particularly unlikely as the least contaminated sample (B62/2) has the highest $^{187}Os/^{188}Os$ isotope ratio. Accordingly, the elevated $^{187}Os/^{188}Os$ ratios of the Rum picrites most probably reflect Os isotope variability of the mantle source.

8.d. Mantle source of the picritic magmas

Kent & Fitton (2000) subdivided the British Palaeogene basaltic magma types of the province on the basis of their Zr/Y, Ti/Zr and Ce/Y ratios, which are insignificantly affected by crustal contamination. Variations in these ratios reflect the different degrees and depths of partial melting and/or differences in source composition. Of the four types (M1–M4) so defined, the Rum picrites equate most closely to the M2 type which is widely represented among the 'Small Isles' of Rum, Eigg, Muck and Canna, although differing from all four types in having lower values for normalized La, Ce and Nd. Other trace element systematics (Nb, Y, Zr) (Fitton *et al.* 1997) are consistent with the picrites having been derived from a depleted mantle source with similarities to a normal MORB-source (Fig. 11).

That the picritic magmas were derived from a depleted source is supported by the REE patterns indicating that the source had experienced LREE depletion, progressive from La to Nd, and also by the high Zr/Nb values suggesting a source previously depleted in Nb. Since a higher concentration of P would be expected in small-fraction melts, the negative P anomalies in these samples might also relate to P loss in an earlier depletion, if it is not a character inherited from the mantle source. The ε_{Nd} of the Rum picrites is indicative of a depleted source distinct from primitive mantle.

It has been proposed that the head of the ancestral Iceland mantle plume was zoned, with an outer sheath of hot ambient (MORB-source) upper mantle surrounding the 'Icelandic source' mantle plume core (Fitton *et al.* 1997; Chambers & Fitton, 2000). In the Mull volcanic centre, to the south of Rum, magmatism commenced at 60 ± 0.3 Ma with magmas arising from MORB-source mantle (Chambers & Fitton, 2000). Some 1.9 m.y. later a change took place after which basalt magmas of Icelandic type were derived from the hypothesized plume core. The youngest basalts of Mull, however, show reversal to MORB-source chem-

https://doi.org/10.1017/S0016756802006684 Published online by Cambridge University Press

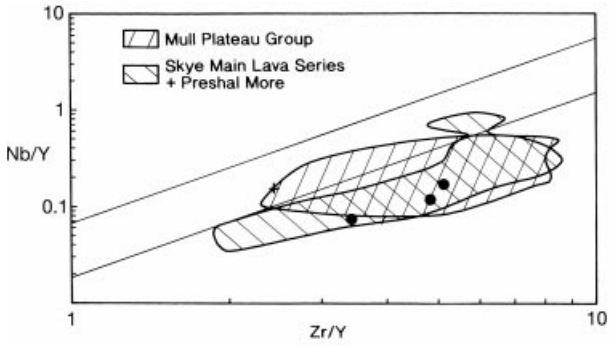

Figure 11. ΔNb diagram (after Fitton *et al.* 1997). Dots indicate data points for the Rum picrites; the cross indicates primitive mantle composition. Data fields for Mull Plateau Group and Skye Main Lava Series + Preshal More from Chambers & Fitton (2000).

istry as the continental plate migrated across the plume axis.

On the basis of this zoned plume-head model, the 60.5 Ma Rum picritic magmas could have arisen from the MORB-source outer sheath of the plume head in the same manner as for the early Mull magmas. However, although the Zr, Nb, Y and high ε_{Nd} of the Rum picrites indicate a MORB-like mantle source, there are a number of characteristics in which they differ from MORB. In particular, the Os isotope variability and certain trace element features of the Rum picrites clearly distinguish them from the MORB reservoir (Fig. 10). These distinctive features include the presence of excess Sr (Sr/Sr* > 1: Table 2, Fig. 7) and deficiency in P (Fig. 7), in addition to the high concentrations of Os and Re (> 1 ppb: Table 3). High concentrations of Os in the Rum picrites are in accordance with the generally high Os concentrations in picrites from flood basalt provinces (e.g. Walker *et al.* 1999; Brooks *et al.* 1999; Schaefer, Parkinson & Hawkesworth, 2000; Larsen & Pedersen, 2000) and are not typical of the MORB reservoir.

The elevated $^{187}Os/^{188}Os$ ratios of the Rum picrites indicate that their source is not North Atlantic MORB mantle (Fig. 10). Rather, the Os systematics of the picrites point towards a time-integrated mantle source with elevated Re/Os ratios. The Rum picrite Nd–Os isotope data are very similar to the depleted component of the Iceland plume (Skovgaard *et al.* 2001), even though they extend the range in $^{187}Os/^{188}Os$ to slightly more radiogenic values.

A mantle source consisting of recycled oceanic lithosphere has been proposed for the recent Iceland picrites (Skovgaard *et al.* 2001). The trace element spectra for recent Iceland picrites (Fig. 7) show several features that clearly distinguish them from MORB. The distinctions include negative anomalies for Nb (relative to La) and for P (relative to Sr and Nd) and positive anomalies for Sr (relative to Ce and Nd) as well as high concentrations of Os (Skovgaard *et al.* 2001).

The high Re content of the Rum picrites accords with the modelling of the REE data indicating that the melts were mainly derived from a garnet lherzolite-facies mantle as Re is compatible in garnet (Righter & Hauri, 1998). One possible explanation for the source being rich in Re is that this element was retained during dehydration or melting during recycling of oceanic lithosphere (Righter & Hauri, 1998). Hence garnet may preserve the high Re/Os ratio of subducted oceanic crust during subduction zone processing and the high Re of the mantle source could imply that the latter consisted of recycled oceanic crust.

Several trace element characteristics and the Os–Nd isotope systematics of the Rum picrites are similar to those of modern Iceland picrites (Skovgaard *et al.* 2001) indicating that they were derived from a depleted component in the Iceland plume. If the three Rum samples reflect the full range of the variability of the mantle source, the temporal evolution of the Iceland plume, as indicated by the Os isotope data from the Rum picrites, suggests that the mantle source has remained remarkably stable and unchanged over the past 60.5 Ma.

9. Conclusions

The Rum magmatism involved high-temperature picritic melts with MgO contents estimated at 18–20 wt%. Olivine macrocrysts with compositions of up to Fo93, highly unusual in Phanerozoic igneous rocks, may have had their Fo contents marginally enhanced by oxidation and/or olivine–spinel interaction.

The Rum magmas represent relatively small-fraction melts of between 5 and 10%, derived mainly from a garnet–lherzolite facies depleted mantle source. Small fraction melts from a depleted source, such as are postulated here, are also highly unusual, melting usually progressing to greater degrees and at shallower (spinel lherzolite facies) depths of separation.

The picrites were slightly modified by small degrees of crustal contamination; on the basis of Sr and Pb isotope data the contamination was < 1% in samples, M9 and B62/2 and ~2.5% in sample B65. The picrites have Os isotope signatures significantly more radiogenic than those of MORB and which are not readily accounted for by assimilation processes. The Os–Nd variation in the least contaminated (M9 and B62/2) samples shows similarity to that of recent Iceland picrites and may indicate that they represent melting of depleted Icelandic mantle plume material.

The idiosyncratic characteristics of the Rum dyke magmas demand unusual conditions for their petrogenesis. We suggest that displacements of the Long Loch Fault may have facilitated partial melting of the newly arisen Iceland plume.

https://doi.org/10.1017/S0016756802006684 Published online by Cambridge University Press

Acknowledgements. Our thanks go to J. G. Fitton & D. James for XRF analyses, to B. Hardarson for Sr and Nd isotope analyses and to N. Walsh for REE analyses. We are grateful to P. Hill for assistance with electron-microprobe analyses and to L.-M. Larsen, B. Schaefer, F. G. F. Gibb, S. Maaløe, I. J. Parkinson and F. Melcher for help and constructive criticism.

References

ARNDT, N.T., LEHNERT, K. & VASIL'EV, Y. 1995. Meimechites: highly magnesian alkaline magmas from the subcontinental lithosphere? *Lithos* **34**, 41–59.

BLICHERT-TOFT, J., ALBARÈDE, F. & KORNPROBST, J. 1999. Lu–Hf systematics of garnet pyroxenites from Beni Bouchera, Morocco: implications for basalt origin. *Science* **283**, 1303–6.

BORTHWICK, J. & HARMON, R. S. 1982. A note regarding ClF_3 as an alternative to BrF_5 for oxygen isotope analysis. *Geochimica et Cosmochimica Acta* **46**, 1665–8.

BROOKS, C. K., KEAYS, R. R., LAMBERT, D. D., FRICK, L. R. & NIELSEN, T. F. D. 1999. Re–Os isotope geochemistry of Tertiary picritic and basaltic mgmatism of East Greenland: constraints on plume–lithosphere interactions and the genesis of the Platinova reef, Skaergaard intrusion. *Lithos* **47**, 107–26.

BROWN, G. M. 1956. The layered ultrabasic rocks of Rhum, Inner Hebrides. *Philosophical Transactions of the Royal Society of London, Ser. B.* no. 668 **240**, 1–53.

BUTCHER, A. R., PIRRIE, D., PRITCHARD, H. M. & FISHER, P. 1999. Platinum-group mineralisation in the Rum layered intrusion, Scottish Hebrides, UK. *Journal of the Geological Society, London* **156**, 213–16.

CHAMBERS, L. M. & FITTON, J. G. 2000. Geochemical transitions in the ancestral Iceland plume: evidence from the Isle of Mull Tertiary volcano, Scotland. *Journal of the Geological Society, London* **157**, 261–3.

CHAUVEL, C. & HÉMOND, C. 2000. Melting of a complete section of recycled oceanic crust: trace element and Pb isotopic evidence from Iceland. *Geochemistry Geophysics Geosystems* **G3** 1 (Feb. 14th).

CLAYTON R. N. & MAYEDA, T. K. 1963. The use of bromine pentafluoride in the extraction of oxygen from oxides and silicates for isotopic analysis. *Geochimica et Cosmochimica Acta* **27**, 43–52.

DANYUSHEVSKY, L. V. & SOBOLEV, A. V. 1996. Ferric–ferrous ratio and oxygen fugacity calculations for primary derived melts: calibration of an empirical technique. *Mineralogy and Petrology* **57**, 229–41.

DICKIN, A. P. 1981. Isotope geochemistry of Tertiary igneous rocks from the Isle of Skye, N.W. Scotland. *Journal of Petrology* **22**, 155–89.

DONALDSON, C. H. 1975. Ultrabasic breccias in layered intrusions – the Rhum Complex. *Journal of Geology* **83**, 33–45. 1976.

DONALDSON, C. H. 1976 An experimental investigation of olivine morphology. *Contributions to Mineralogy and Petrology* **57**, 187–213.

DROOP, G. T. R. 1987. A general equation for estimating Fe^{3+} concentration in ferromagnesian silicates and oxides from microprobe analyses using stoichiometric criteria. *Mineralogical Magazine* **51**, 431–6.

EMELEUS, C. H. 1997. Geology of Rum and the adjacent islands. *Memoir for 1:50 000 Geological Sheet 60 (Scotland)*. British Geological Survey, 170 pp. London: The Stationery Office.

EMELEUS, C. H., CHEADLE, M. J., HUNTER, R. H., UPTON, B. G. J., & WADSWORTH, W. J. 1996. The Rum Layered Intrusion. In *Layered Intrusions* (ed. C. G. Cawthorn), pp. 331–63. Elsevier Science B.V.

ESSER, B. K. & TUREKIAN, K. K. 1993. The osmium isotopic composition of the continental crust. *Geochimica et Cosmochimica Acta* **57**, 3093–3104.

FAITHFULL, J. W. 1985. The Lower Eastern Layered Series of Rhum. *Geological Magazine* **122**, 459–68.

FITTON, J. G., SAUNDERS, A. D., LARSEN, L.-M., HARDARSON, B. S. & NORRY, M. J. 1998. Volcanic rocks from the southeast Greenland margin at 63°N: composition, petrogenesis and mantle sources. In *Proceedings of ODP Scientific Results 152* (eds A. D. Saunders, H. C. Larsen and S. H. Wise), pp. 331–50. College Station, TX.

FITTON, J. G., SAUNDERS, M. J., NORRY, M. J., HARDARSON, B. S. & TAYLOR, R.N. 1997. Thermal and chemical structure of the Iceland plume. *Earth and Planetary Science Letters* **153**, 197–208.

FORD, C. E., RUSSELL, D. G., CRAVEN, J. A. & FISK, M. R. 1983. Olivine–liquid equilibria: temperature, pressure, and composition dependence of the crystal/liquid partition coefficients for Mg, Fe^{2+}, Ca, and Mn. *Journal of Petrology* **24**, 256–65.

FRANCIS, D. 1985. The Baffin Bay lavas and the value of picrites as analogues of primary magmas. *Contributions to Mineralogy and Petrology* **89**, 144–54.

FREI, R. & ROSING, M. 2001. The least radiogenic terrestrial leads; implications for the early Archaean crustal evolution and hydrothermal–metasomatic processes in the Isua Supracrustal Belt (West Greenland). *Chemical Geology* **181**, 47–66.

GALLAGHER, M. J., BASHAM, I. R. & 10 OTHERS. 1989. Marine deposits of chromite and olivine, Inner Hebrides of Scotland. *British Geological Survey Technical Report, WF/89/13. British Geological Survey*: Mineral Reconnaissance Programme Report, no. 106, 20 pp.

GARCIA, M. O., HULSEBOSCH, T. P. & RHODES, J. M. 1995. Geochemistry of the 1852 and 1868 picrites: clues to parental magma compositions and the magmatic plumbing. In *Mauna Loa revealed: structure, composition, history and hazards* (eds J. M. Rhodes & J. P. Lockwood), pp. 219–39. Geophysical Monograph no. 92, American Geophysical Union, Washington, D.C.

GIBB, F. G. F. 1976. Ultrabasic rocks of Rhum and Skye: the nature of the parent magma. *Journal of the Geological Society, London* **132**, 209–22.

GOVINDARAJU, K. 1994. 1994 compilation of working values and sample description for 383 geostandards. *Geostandards Newsletter* **18**, 1–158.

GREENWOOD, R. C., DONALDSON, C. H. & EMELEUS, C. H., 1990. The contact zone of the Rum ultrabasic intrusion: evidence of peridotite formation from magnesian magmas. *Journal of the Geological Society, London* **147**, 209–12.

HAGGERTY, S. E. & BAKER, I. 1967. The alteration of olivine in basaltic and associated lavas. 1. High temperature alteration. *Contributions to Mineralogy and Petrology* **17**, 233–57.

HAMILTON, M. A., PEARSON, D. G., THOMPSON, R. N., KELLEY, S. P. & EMELEUS, C. H. 1998. Rapid eruption of Skye lavas inferred from precise U–Pb and Ar–Ar dating of the Rum and Cuillin plutonic complexes. *Nature* **394**, 260–3.

Henderson, P. & Gijbels, R. 1976. Trace element indicators of the Rhum layered intrusion, Inner Hebrides. *Scottish Journal of Geology* **12**, 325–33.

Hirschmann, M. M. & Stolper, E. M. 1996. A possible role for garnet pyroxenite in the origin of the "garnet signature" in MORB. *Contributions to Mineralogy and Petrology* **124**, 185–208.

Kamenetsky, S. S., Crawford, A. J. & Meffre, S. 2001. Factors controlling chemistry of magmatic spinel: an empirical study of associated olivine, Cr-spinel and melt inclusions from primitive rocks. *Journal of Petrology* **42**, 655–71.

Kent, R. W., 1995. Magnesian basalts from the Hebrides, Scotland; chemical composition and relationship to the Iceland plume. *Journal of the Geological Society, London* **152**, 979–83.

Kent, R. W. & Fitton, J. G. 2000. Mantle sources and melting dynamics in the British Palaeogene Igneous Province. *Journal of Petrology* **41**, 1023–40.

Kitchen, D. E. 1985. The parental magma on Rhum: evidence from alkaline segregations and veins in the peridotites from Salisbury's Dam. *Geological Magazine* **122**, 529–37.

Klemme, S. & O'Neill, H. St C. 2000. The near-solidus transition from garnet lherzolite to spinel lherzolite. *Contributions to Mineralogy and Petrology* **138**, 237–48.

Larsen, L. M. & Pedersen, A. K. 2000. Processes in high-Mg, high-T magmas: evidence from olivine, chromite and glass in Palaeogene picrites from West Greenland. *Journal of Petrology* **41**, 1071–98.

LeBas, M. J. 2000. IUGS reclassification of the high-Mg and picritic volcanic rocks. *Journal of Petrology* **41**, 1467–70.

Li, J.-P., O'Neill, H. St C. & Seifert, F. 1995. Subsolidus phase relations in the system MgO–SiO_2–Cr-O in equilibrium with metallic Cr, and their significance for the petrochemistry of chromium. *Journal of Petrology* **36**, 107–32.

Maurel, C. & Maurel, P. 1982. Etude experimentale de l'equilibre Fe^{2+}–Fe^{3+} dans les spinelles chromiferes et les liquides silicates basiques coexistants à 1 atm. *Comptes Rendus Academie des Sciences, Paris* **285**, 209–15.

McDonough, W. F. & Sun, S.-s. 1995. The composition of the Earth. *Chemical Geology* **120**, 223–53.

McKenzie, D. P. & O'Nions, R. K. 1991. Partial melt distributions from inversion of rare earth element concentrations. *Journal of Petrology* **32**, 1021–91.

Nägler, T. F. & Frei, R. 2001. "Plug in" Os distillation. *Schweizerische Mineralogische und Petrographische Mitteillungen* **77**(1), 123–7.

Norrish, K. & Hutton, J. T. 1969. An accurate spectrographic method for the analysis of a wide range of geological samples. *Geochimica et Cosmochimica Acta* **33**, 431–53.

Palacz, Z. A. 1985. Sr–Nd–Pb isotopic evidence for crustal contamination in the Rhum intrusion. *Earth and Planetary Science Letters* **74**, 35–44.

Parkinson, I. J., Hawkesworth, C. J. & Cohen, A. S. 1998. Ancient mantle in a modern arc: Osmium isotopes in Izu-Bonin-Mariana forearc peridotites. *Science* **281**, 2011–13.

Peuker-Ehrenbrink, B. & Jahn, B-M. 2001. Rhenium–osmium isotope systematics and platinum group element concentrations: Loess and the upper continental crust. *Geochemistry Geophysics Geosystems* **2**, (Oct. 22), Paper no. 2001GC000172.

Révillon, N. T., Arndt, N. T., Chauvel, C. & Hallot, E. 2000. Geochemical study of ultramafic volcanic and plutonic rocks from Gorgona Island, Columbia: the plumbing system of an oceanic plateau. *Journal of Petrology* **41**, 1127–53.

Righter, K. & Hauri, E. H. 1998. Compatibility of rhenium in garnet during mantle melting and magma genesis. *Science* **280**, 1737–41.

Roy-Barman, M. & Allègre, J.-C. 1994. $^{187}Os/^{186}Os$ ratios of mid-ocean ridge basalts and abyssal peridotites. *Geochimica et Cosmochimica Acta* **58**, 5043–54.

Saunders, A. D., Fitton, J. G., Kerr, A. C., Norry, M. J. & Kent, R. W. 1997. The North Atlantic Igneous Province. In *Large Igneous Provinces* (eds J. J. Mahoney and M. F. Coffin), pp. 45–94. Geophysical Monograph no. 100. Washington, D.C.: American Geophysical Union.

Schaefer, B. F., Parkinson, I. J. & Hawkesworth, C. J. 2000. Deep mantle plume osmium isotope signature from West Greenland Tertiary picrites. *Earth and Planetary Science Letters* **175**, 105–18.

Shirey, S. B. & Walker, R. J. 1998. The Re–Os isotope system in cosmochemistry and high temperature geochemistry. *Annual Review of Earth and Planetary Science Letters* **26**, 423–500.

Skovgaard A. C., Storey, M., Baker, J., Blusztajn, J. & Hart, S. R. 2001. Osmium–oxygen isotope evidence for a recycled and highly depleted component in the Iceland plume. *Earth and Planetary Science Letters* **194**, 259–75.

Snow, J. E. & Reisberg, L. 1995. Os isotopic systematics of the MORB mantle: results from altered abyssal peridotites. *Earth and Planetary Science Letters* **133**, 411–21.

Speight J. M., Skelhorn, R. R., Sloan, T. & Knaap, R. J. 1982. The dyke swarms of Scotland. In *Igneous Rocks of the British Isles* (ed. J. S. Sutherland), pp. 449–59. Chichester: John Wylie & Sons.

Sweatman, T. R. & Long, J. V. P. 1969. Quantitative electron microanalysis of rock-forming minerals. *Journal of Petrology* **10**, 332–79.

Thirlwall, M. F. 1995. Generation of Pb isotopic characteristics of the Iceland plume. *Journal of the Geological Society, London* **152**, 991–6.

Thirlwall, M. F., Upton, B. G. J. & Jenkins, C. 1994. Interaction between continental lithosphere and the Iceland Plume – Sr–Nd–Pb isotope geochemistry of Tertiary basalts, NE Greenland. *Journal of Petrology* **35**, 839–79.

Thompson, R. N. 1982. Magmatism of the British Tertiary Volcanic Province. *Scottish Journal of Geology* **18**, 49–107.

Thompson, R. N. & Gibson, S.A. 2000. Transient high temperatures in mantle plume heads inferred from magnesian olivines in Phanerozoic picrite. *Nature* **407**, 502–5.

Todt, W., Cliff, R. A., Hanser, A. & Hoffman, A. W. 1993. Recalibration of NBS lead standards using a ^{202}Pb + ^{205}Pb double spike. *Terra Abstract* (Suppl. 1), 596.

Troll, V. R., Emeleus, C. H. & Donaldson, C. H. 2000. Caldera formation in the Rum Central Igneous Complex, Scotland. *Bulletin of Volcanology* **62**, 301–17.

Ulmer, P. 1989. The dependence of the Fe^{2+}–Mg cation-partitioning between olivine and basaltic liquid on pressure, temperature and composition. An experimental

study to 30 kbars. *Contributions to Mineralogy and Petrology* **101**, 261–73.

UPTON, B. G. J., ASPEN, P. & HINTON, R. W. 2001. Pyroxenite and granulite xenoliths from beneath the Scottish Northern Highlands Terrane: evidence for lower crust/upper mantle relationships. *Contributions to Mineralogy and Petrology* **142**, 178–97.

VOLKER, J. A. & UPTON, B. G. J. 1990. The structure and petrogenesis of the Trallval and Ruinsival areas of the Rhum ultrabasic complex. *Philosophical Transactions of the Royal Society of Edinburgh, Earth Sciences* **81**, 69–88.

WADSWORTH, W. J. 1994. The peridotite plugs of northern Rum *Scottish Journal of Geology* **30**, 167–74.

WALKER, R. J., STOREY, M., KERR, A. C., TARNEY, J. & ARNDT, N. T. 1999. Implications of ^{187}Os isotopic heterogeneities in a mantle plume: Evidence from Gorgona Island and Curaçao. *Geochimica et Cosmochimica Acta* **63**, 713–28.

WALSH, N. M., BUCKLEY, F. & BARKER, J. 1981. The simultaneous determination of the rare-earth elements in rocks using inductively coupled plasma source spectrometry. *Chemical Geology* **33**, 141–53.